Journal of Power Sources 230 (2013) 143–147

Contents lists available at SciVerse ScienceDirect

Journal of Power Sources

journal homepage: www.elsevier.com/locate/jpowsour

Short communication

Cyclic Capacity Fade Plots for aging studies of Li-ion cells

M.M. Joglekar, N. Ramakrishnan*

India Science Lab, GM Global R&D, General Motors Technical Centre India Pvt. Ltd., Bangalore 560066, India

HIGHLIGHTS

- Proposes two types of quick-reference plots to illustrate cyclic life of Li ion battery material.
- '% Capacity loss/cycle' vs. '$(SOC_{max} - SOC_{min})^*(SOC_{mean})$' show monotonic variation.
- '$(SOC_{max} - SOC_{min})(SOC_{mean})$' vs. 'Log (%Capacity loss/cycle)' also exhibits similar feature.
- Demonstrated for different material & temperature combinations.
- In the above cases, the applicability of linear trend is also quantified.

ARTICLE INFO

Article history:
Received 8 November 2012
Received in revised form
12 December 2012
Accepted 15 December 2012
Available online 22 December 2012

Keywords:
Lithium ion cell
Aging
Cyclic capacity fade
Design plots

ABSTRACT

The article introduces a Cyclic Capacity Fade Plot, to depict the deterioration of a lithium-ion cell material, as a graph between a factor based on State of Charge (ΔSOC^*SOC_{mean}) and the % capacity loss per cycle. The plots are generated entirely using experimental data. A variant of this plot is presented as Log(cycle life) vs. ΔSOC^*SOC_{mean}, that is analogous to Stress–Number of Cycles (*S–N*) type limit curves used in the study of cyclic fatigue of metallic materials. The monotonic variation and in some cases near linear nature of these plots, valid for different temperatures, is noteworthy. These plots provide a wealth of information at a quick glance and are shown to be useful in comparing the performance of different cell materials. The utility of the Cyclic Capacity Fade Plots is demonstrated illustratively for two (Li Manganese Oxide) LMO-graphite cells studied in-house and for an olivine system reported in the literature. These plots are expected to be useful in electrode material development, accelerated testing, battery health management etc.

1. Introduction

In the last two decades, the research and development activities associated with battery performance, mainly due to the applications in electric vehicles and mega energy storage systems, is witnessing a great progress. The details can be found in review articles [1–3]. In this context, the engineering and the design community involved in these activities need quick reference tools especially for making critical decisions. Plots, which provide a snap shot of design or engineering information at a quick glance, have already been in practice for different applications in the disciplines of Materials, Mechanical, Aerospace, Civil Engineering, etc. This investigation introduces a concept for one such Plot for depicting cyclic aging of Li ion batteries. In this presentation, we call it 'Cell Material Cyclic Capacity Fade Plot' (CCFP).

The inspiration to generate the CCFP comes from Stress–Number of Cycles (*S–N*) curves [4] that are commonly used in the field of metal fatigue. Just for the reader's convenience, a set of *S–N* curves of steel and Aluminum is shown in Fig. 1. Here, life of the material under structural fatigue loading is measured in terms of the number of cycles it can sustain and the cycle life depends on a stress measure. Below a particular critical stress, referred to as endurance limit, the cycle life is expected to be infinity for structural steel while such a clear demarcation doesn't exist for other materials such as Aluminum. The fatigue strength in the case of Aluminum is identified as the number of cycles it can sustain without failure if operated at a certain stress level. In similar lines, Verbrugge and Cheng [5] suggested ΔSOC (Change in State of Charge ie $SOC_{max} - SOC_{min}$) as the parameter of measure for cycle life for Li-ion battery electrode materials since ΔSOC directly corresponds to the intercalation induced stress. In this investigation, we found ΔSOC^*SOC_{mean} $[(SOC_{max} - SOC_{min})^*(SOC_{max} + SOC_{min})/2]$ to be a better measure

* Corresponding author. Present address: M S Ramiah School of Advanced Studies, Bangalore 560058, India. Tel.: +91 9008011844 (mobile).
E-mail addresses: ramkrish@sify.com, ramkrish0123@gmail.com (N. Ramakrishnan).

0378-7753/$ – see front matter © 2012 Elsevier B.V. All rights reserved.
http://dx.doi.org/10.1016/j.jpowsour.2012.12.060

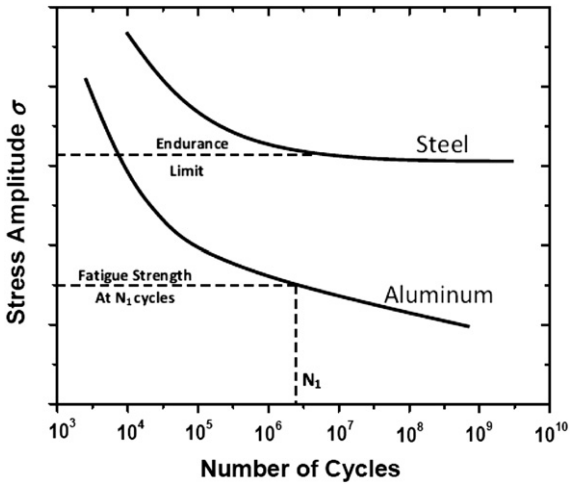

Fig. 1. Typical endurance limit (metal fatigue) curves pertaining to cycle life of steel and aluminum.

and the details are given in the following sections. One such plot relating the cycle life and the stoichiometric variation of lithium in a Li compound was presented by Delmas and Capitaine [6]. The objective of the Capacity Fade Plots is to offer an idea about the cycle life of a typical battery electrode material at a quick glance.

2. Cell Material Cyclic Capacity Fade Plots

2.1. Experimental data

Two chemically variant (Li Manganese Oxide) LMO-Graphite based cells, referred to as Cell A and Cell B in this presentation were tested for cyclic degradation. The tests were carried out in accordance with USABC test protocol [7]. Both the cells were subjected to charge–discharge cycles and the capacity-fade was monitored at selected intervals during cycling. The performance of the cells after specified cycles, including an uncycled one, is established in terms of voltage–capacity discharge curves. This is known as Reference Performance Test (RPT) discharge curve. A typical voltage–discharge curve resulting from the RPT of a cell is shown in Fig. 2a. The end-of-charge voltage (EOCV) for the RPT was set to 4.14 V, while the end-of-discharge voltage was set to 3 V. The total capacity drop in an uncycled cell at 3 V is treated as 100% capacity dischargeable. A cycle comprises a set of representative profiles of charge–discharge processes, which is experienced in real service conditions, known as Dynamic Stress Test (DST). A typical segment of DST comprises the constant power charge/discharge processes spanning over a time interval and in this case it is 360 s. When the cell undergoes these charge/discharge cycles, the State of Charge (SOC) of the cell is changed. In each experiment, the upper and the lower SOCs of the cell are maintained. Beginning the experiment with SOC_{max}, multiple segments of DST profiles are operated to reach the SOC_{min}. An illustrative plot is presented in Fig. 2b, where two ΔSOC cases are shown. The plots in Fig. 2b are generated using voltage–discharge and DST data. As can be seen, the effective charge/discharge rate during the cycling is around 2C. At intervals of about 200 cycles, RPTs are carried out to observe the capacity loss.

Table 1
Experimental study of seven combinations of ΔSOC*SOC.

No.	SOC_{max}	SOC_{min}	$\Delta SOC = SOC_{max} - SOC_{min}$	$SOC_{mean} = 0.5^*(SOC_{max} + SOC_{min})$	ΔSOC^*SOC_{mean}
1	1.00	0.25	0.75	0.625	0.47
2	1.00	0.40	0.60	0.70	0.42
3	1.00	0.50	0.50	0.75	0.38
4	0.85	0.25	0.60	0.55	0.33
5	0.75	0.25	0.50	0.50	0.25
6	0.75	0.45	0.30	0.60	0.18
7	0.75	0.65	0.10	0.70	0.07

In this investigation, seven different combinations of upper and lower SOC were considered for carrying out the cyclic test for each of the three temperatures. Table 1 contains the values of the upper and the lower SOC levels corresponding to each of the seven cases. These seven cases are repeated for three different temperatures (20 °C, 35 °C, and 50 °C) amounting to a total of 21 experimental datasets each for Cell A and Cell B.

2.2. The parameter ΔSOC^*SOC_{mean}

In this investigation, we arrived at an SOC based lumped parameter ΔSOC^*SOC_{mean} as a key measure of charge–discharge cyclic fatigue experienced by a cell. The condensed and simplified form of the derivation is presented in Appendix-A and the detailed

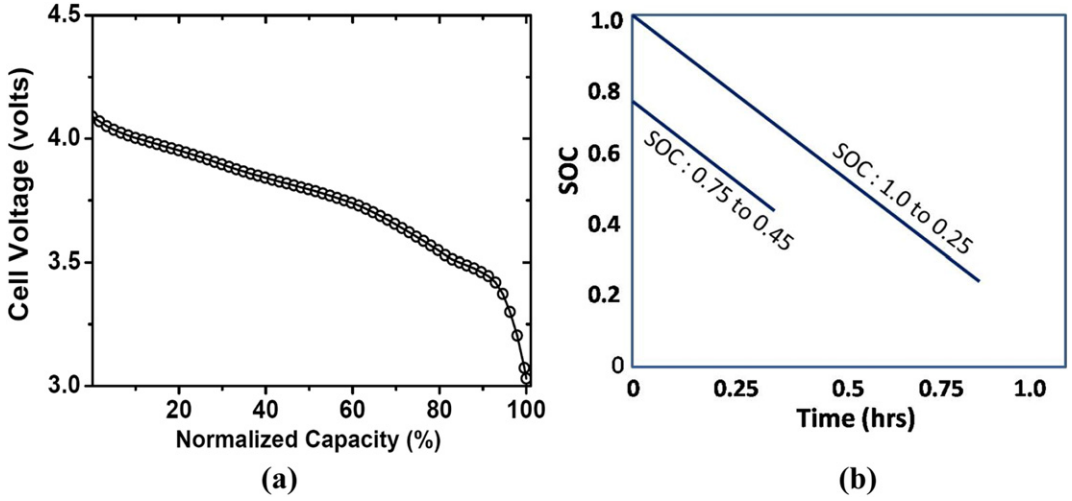

Fig. 2. (a) A typical Reference Performance Test (RPT) discharge curve of a pristine cell (b) typical variation of SOC during two representative cyclic experiments determined based on the DST.

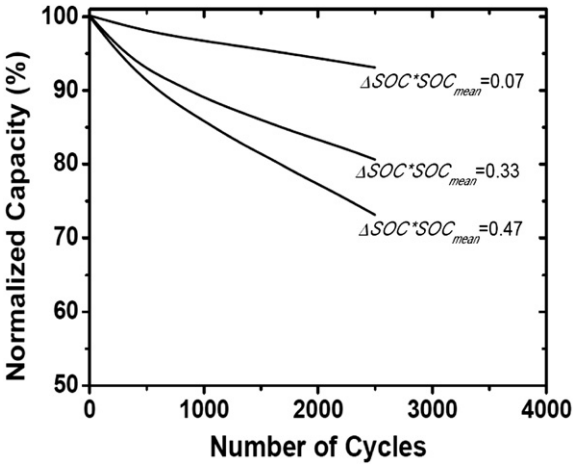

Fig. 3. Capacity retention plot of cell A for a range of $\Delta SOC^{*}SOC_{mean}$ levels (minimum, intermediate and maximum from those specified in Table 1) for 35 °C.

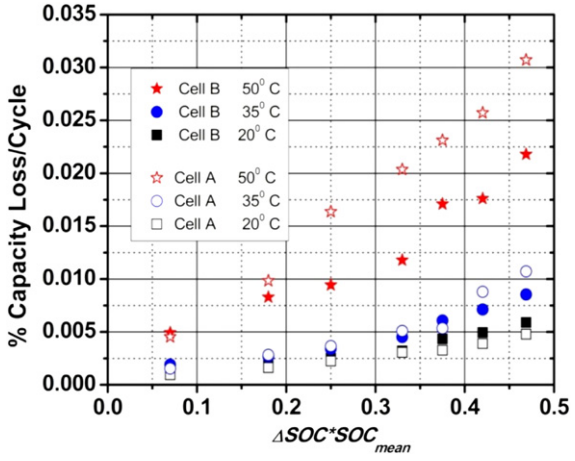

Fig. 4. % Capacity loss/cycle vs. $\Delta SOC^{*}SOC_{mean}$ for cells A and B.

presentation can be found in the earlier work [5,8,9]. The factor $\Delta SOC^{*}SOC_{mean}$ directly corresponds to the average strain energy that the electrode material experiences during the entire course of a cycle. This is analogous to the expressions employed to characterize metal fatigue. We can heuristically argue that ΔSOC is analogous to the stress band of the fatigue and SOC_{mean} is to the mean stress associated with metal fatigue [4]. The maximum value of $\Delta SOC^{*}SOC_{mean}$ is 0.5 and the minimum is 0.

2.3. Construction of the Cyclic Capacity Fade Plots

The basic data for constructing the capacity fade plots is extracted from the capacity retention curves and one such set of plots is presented in Fig. 3 for illustration. The average capacity loss per cycle is computed for 21 different combinations of $\Delta SOC^{*}SOC_{mean}$ and temperatures. The definition of 'Failure' becomes critical here. To the best of the authors' knowledge, no established quantitative definition for failure exists in the context of battery electrodes. For the cases considered in the present analysis, we assumed the end of life to correspond to 60% of the capacity loss at 3 V.

In the case of cyclic degradation, there is a steep voltage drop at the beginning of the capacity fade curves because of the SEI (Solid Electrolyte Inter-phase) formation on the electrode particle surfaces but later stabilizes to a near linear variation. For all practical purposes, the dependence of capacity retention curves on number of cycles can be assumed to be linear in cyclic degradation. Fig. 4 shows experimentally determined values of % capacity loss per cycle vs. $\Delta SOC^{*}SOC_{mean}$, for Cell A and Cell B. In addition, the data can be plotted similar to the *S–N* type endurance limit curves (cyclic fatigue life) of metallic materials. Fig. 5a shows a plot representing the cycle life expressed in terms of $\Delta SOC^{*}SOC_{mean}$ and temperature, for Cell A and Cell B. It is interesting to note that the plots (Fig. 5b) exhibit a monotonic variation. It exhibits near linearity, when 'Log(cycle life)' is considered on *x*-axis instead of 'cycle' life itself. This demonstrates the possibility of existence of *S–N* type durability curves for Li ion batteries as suggested by Verbrugge and Cheng [5].

3. Discussion

Primarily, the experimental points plotted as $\Delta SOC^{*}SOC_{mean}$ vs. % capacity loss per cycle exhibit a monotonically varying trend, providing a quick comprehension of the aging process. As a preliminary approximation, the best fit straight lines of the points shown in Fig. 4 are drawn for each temperature (20 °C, 35 °C, and 50 °C) in Fig. 6a–c for Cell A and Cell B. The best-fit parameters are shown on the respective plots. The values of the correlation coefficients in each case substantiate the choice of the linear fit except

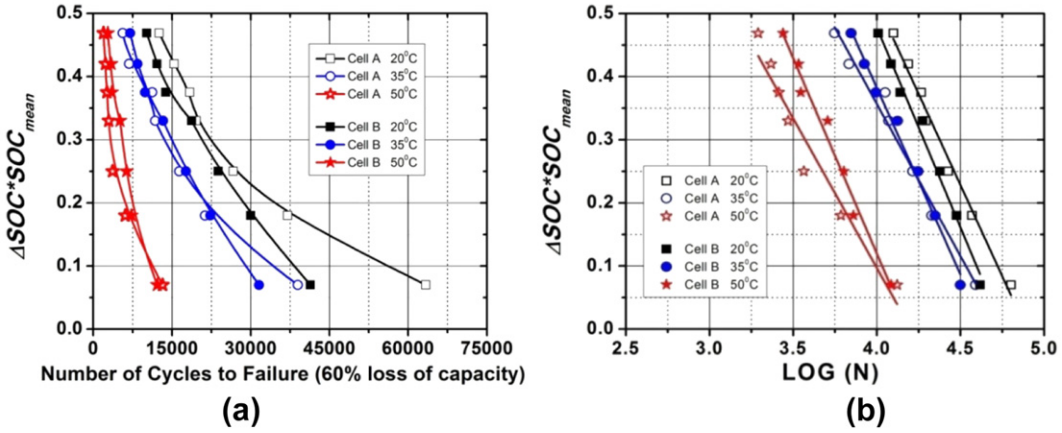

Fig. 5. Cycle life expressed in terms of $\Delta SOC^{*}SOC_{mean}$ for different temperatures – similar to *S–N* type durability curves of metal fatigue (a) life expressed in terms of *N* (b) life expressed in terms of Log(*N*).

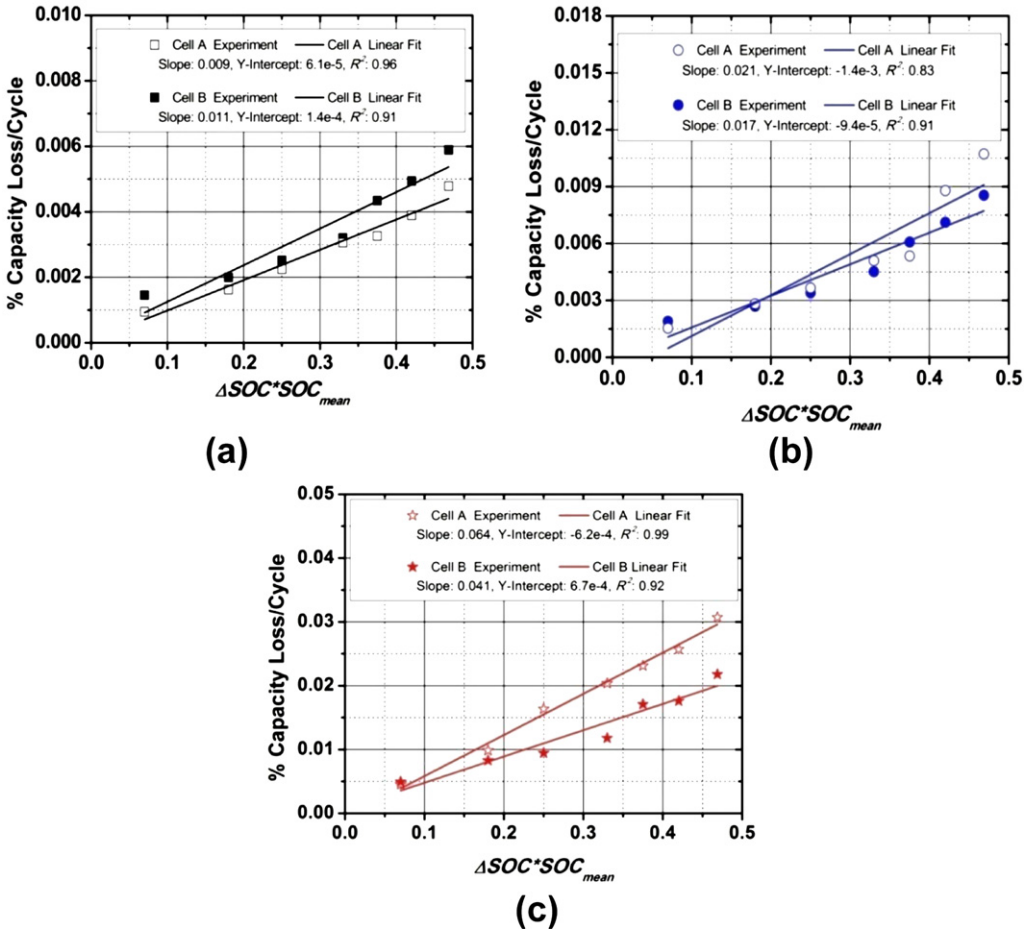

Fig. 6. Capacity fade plot of the data shown in Fig. 4 in a linearized form: (a) 20 °C (b) 35 °C (c) 50 °C corresponding to cells A and B.

the one corresponding to Cell A in Fig. 6b. The idea here is not to impose the linearity but to show how best the linearity assumption works. The studies conducted on Cell A and Cell B reveal that there is no significant threshold value of $\Delta SOC^{*}SOC_{mean}$ below which the life can be considered to be limitless. In these cases, only when $\Delta SOC^{*}SOC_{mean} \sim 0$, the rate of capacity fade vanishes which can be seen in the *y*-intercepts in Fig. 6a and c. The resolution of the plots appears to be sufficient that it can be used for comparing the performance of two cells. Cell A has lower % capacity loss compared to Cell B at 20 °C. The trend gets reversed at 50 °C. Similarly, the performance of Cell A is better at low $\Delta SOC^{*}SOC_{mean}$ value compared to Cell B and the trend is reversed at higher values of $\Delta SOC^{*}SOC_{mean}$.

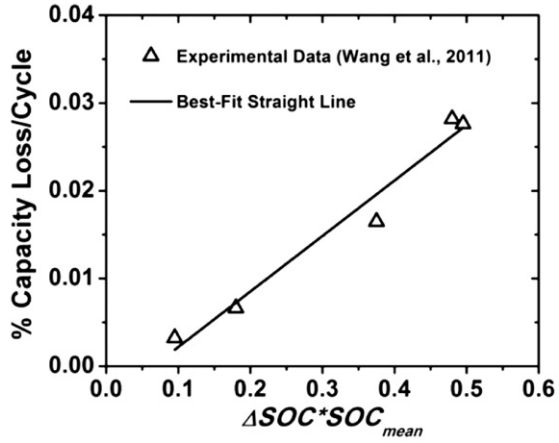

Fig. 7. Cyclic Capacity Fade Plot for the data reported by Wang et al. [10].

In addition to our own data, we considered a study reported by Wang et al. [10] in order to confirm the applicability of Cyclic Capacity Fade Plots for different materials. The data [10] pertains to Graphite–$LiFePO_4$ system. We used the capacity retention data pertaining to cycling at 60 °C, C/2 rate and various levels of ΔSOC from [10]. We made an attempt to represent this data on %capacity loss/cycle vs. $\Delta SOC^{*}SOC_{mean}$ space which is shown in Fig. 7. It is interesting to see that the data points of Wang et al. [10] also follow a monotonic trend of variation. Unlike the earlier cases pertaining to Cell A & B, the linear plot of the above case [10] intersects the *x*-axis ($\Delta SOC^{*}SOC_{mean}$) at a significant value indicating a threshold value of $\Delta SOC^{*}SOC_{mean}$ below which the capacity loss vanishes. This aspect is somewhat analogous to the case of steel where there is a definite fatigue limit as in Fig. 1. Further investigations are necessary to confirm the existence of such threshold values and the linearity assumption. In addition, the applicability of the concept of the capacity fade plots for SOC_{min} <25% is yet to be ascertained.

4. Conclusions

The investigation establishes a concept for generating 'Cyclic Capacity Fade Plot' using experimental data. This is to depict the cyclic deterioration of a typical aging battery electrode, as a graph

between $\Delta SOC^{*}SOC_{mean}$ and the % capacity loss per cycle. A variant of this plot is presented as a function of Log (cycle life) vs. $\Delta SOC^{*}SOC_{mean}$, similar to the *S–N* type durability curves used in cyclic fatigue of metallic materials. Interestingly, some of the plots exhibit near linearity for all the three temperatures considered. These quick-glance ready reference plots are shown to be useful in comparing different cell materials also. The Cyclic Fade Plots are demonstrated illustratively for two variants of LMO-Graphite based energy cell systems and also for a case reported in the literature. These plots are expected to be useful in electrode material development, accelerated testing and battery health management. Also, the study proposes an SOC based measure ($\Delta SOC^{*}SOC_{mean}$) for characterizing cyclic aging.

Acknowledgments

The authors are thankful to Mark Verbrugge, Sudhakar Inguva for valuable discussions and suggestions. The work was carried out on GM Funding.

Appendix A

For a spherical system, the radial and the tangential strains (ε_r & ε_t) are expressed as,

$$\varepsilon_r = \frac{\partial u}{\partial r} = \frac{1}{E}(\sigma_r - 2\nu\sigma_t) + \frac{1}{3}\gamma C \tag{A.1}$$

$$\varepsilon_t = \frac{u}{r} = \frac{1}{E}(\sigma_t - 2\nu\sigma_r) + \frac{1}{3}\gamma C \tag{A.2}$$

where, u and r are displacement and radial location respectively; E and ν are Young's Modulus and Poisson's ratio; σ is stress, γ is the molar volume expansion due to the intercalation of 1 mol of Li ions and C is the concentration of Li ions. Analogous to thermal analysis, the stress free volume strain 'γC' is included in Eqs. (A1) & (A2). The equilibrium equation is,

$$\frac{d\sigma_r}{dr} + \frac{2(\sigma_r - \sigma_t)}{r} = 0 \tag{A.3}$$

Combining Eqs. (A.1)–(A.3) we get,

$$\frac{d^2u}{dr^2} + \frac{2}{r}\frac{du}{dr} - 2\frac{u}{r^2} = \frac{1}{3}\gamma\frac{(1+\nu)}{(1-\nu)}\frac{dC}{dr} \tag{A.4}$$

For algebraic convenience, we assume a simpler concentration profile in the range $r = 0$ to R to be,

$$C = C_0 + (C_R - C_0)\left(\frac{r}{R}\right)^{\alpha} \tag{A.5}$$

α describes the concentration profile where the concentration at the surface and the center are C_R and C_0 respectively. $\alpha = \infty$ and $\alpha = 0$ correspond to the initial and the final conditions. Eqs. (A.4) and (A.5) yields,

$$\sigma_r - \sigma_t = \sigma_{eff} = \frac{E\gamma}{3(1-\nu)}\frac{\alpha(C_R - C_0)}{(\alpha+3)}\left(\frac{r}{R}\right)^{\alpha} \tag{A.6}$$

Here σ_{eff} is the effective stress at a location r, at any particular instant of charging. Therefore, assuming elastic conditions, the specific strain energy (ψ) is,

$$\psi = \frac{1}{2}\frac{\sigma_{eff}^2}{E} = E\left(\frac{\gamma}{3(1-\nu)}\right)^2\left(\frac{\alpha(C_R - C_0)}{(\alpha+3)}\right)^2\left(\frac{r}{R}\right)^{2\alpha} \tag{A.7}$$

Based on eqn (A.7), we hypothesized $d\psi/dC \propto C$. Over an entire cycle, the average effect of the Li ion concentration, where the concentration varies from SOC_{min} to SOC_{max} and all the other material and geometrical variables remain constant, it can be written

$$\psi \propto \int_{SOC_{min}}^{SOC_{max}} C dC \tag{A.8}$$

Eqn (A.8) yields the factor $\Delta SOC^{*}SOC_{mean}$. Similarly it can be shown that stress corresponds to ΔSOC.

References

[1] P.G. Bruce, S.A. Freunberger, L.J. Hardwick, J.-M. Tarascon, Nat. Mater. 11 (2012) 19–29.
[2] B. Scrosati, J. Garche, J. Power Sources 195 (2010) 2419–2430.
[3] J.W. Fergus, J. Power Sources 195 (2010) 939–954.
[4] G.E. Dieter, D. Bacon, Mechanical Metallurgy, McGraw-Hill Book Company, 1988.
[5] M.W. Verbrugge, Y.T. Cheng, J. Electrochem. Soc. 156 (11) (2009) A927–A937.
[6] C. Delmas, F. Capitaine, in: 8th International Meeting of Lithium Batteries Nagoya, Japan 1996, Extended Abstracts 470–471.
[7] USABC Electric Vehicle Battery Test Procedures Manual, Available on: http://www.uscar.org.
[8] N. Ramakrishnan, M.M. Joglekar, S. Inguva, J. Electrochem. Soc. 160 (1) (2013) A125–A137 (in print).
[9] S.K. Vanimisetti, N. Ramakrishnan, Proc. Mech. Eng. C J. Mech. Eng. Sci. 226 (9) (2012) 2192–2214.
[10] J. Wang, P. Liu, J. Hicks-Garner, E. Sherman, S. Soukiazian, M. Verbrugge, H. Tataria, J. Musser, P. Finamore, J. Power Sources 196 (2011) 3942–3948.